

## Use of a transient model to simulate fluidized bed incineration of sewage sludge

B. Khiari<sup>a,b</sup>, F. Marias<sup>b,\*</sup>, F. Zagrouba<sup>c</sup>, J. Vaxelaire<sup>b</sup>

<sup>a</sup> *Institut National de Recherche Scientifique et Technique, B.P. 95, 2050 Hammam-Lif, Tunisia*

<sup>b</sup> *Laboratoire de Thermique Energétique et Procédés (EA 1932), Université de Pau et des Pays de l'Adour, Rue Jules Ferry, BP 7511, 64075 Pau cedex, France*

<sup>c</sup> *Institut Supérieur des Sciences et Technologies de l'Environnement B.P. 95, 2050 Hammam-Lif, Tunisia*

Received 22 September 2005; received in revised form 16 November 2005; accepted 17 November 2005

Available online 6 January 2006

### Abstract

This paper presents a mathematical model dedicated to fluidized bed incineration of sludge. The main assumptions as well as the principal equations of the model are presented. Basically, this model relies on instantaneous pyrolysis of sludge and on a five zones description of the hydrodynamics into the incinerator. Its originality is essentially due to the introduction of a two-dimensional buffer zone between the bubble and the emulsion phase. The chemistry of the gaseous system is described by chemical equilibrium. Results of a start up procedure have been presented in order to illustrate the ability of the model to describe transient behavior. To validate the model from an energetic point of view, different types of sludge (primary, activated and digested) have been computed and compared to industrial data and to results obtained from a simple calculation. The lower dryness limit corresponds to self incineration of the sludge. The higher one corresponds to maximal thermal level that should not be exceeded within the furnace.

© 2005 Elsevier B.V. All rights reserved.

**Keywords:** Modeling; Fluidized bed; Incineration; Sludge

### 1. Introduction

One of the main drawbacks of wastewater treatment processes (either urban or industrial) is the by-production of sludge. As an example, approximately 9 Mt of sludge (expressed in dry matter) were produced in Europe in 1998 [1]. Up to now, landfill was playing a major role in the disposal of these wastes. However, because of the public awareness of environmental issues as well as European regulation, other treatments have to be used for their processing. Among these processes, one issue is to burn the sludge in incinerator (in 1998, 1 Mt, dry matter, has been burnt all over Europe in 1998 [1]) using either specific furnaces or municipal solid waste incinerators for co-incineration. Although it is a convenient way to reduce the volume and mass of the incoming fluxes, and to a lower extent, to recover energy, incineration has to be highly controlled in order to make it a clean tech-

nology, compatible with sustainable development. To enhance the knowledge about the complexes processes that occur within such devices, and to improve their mode of operation, accurate mathematical models are required in order to predict temperature and composition profiles inside incinerators as well as at their outputs.

Because fluidized beds (Fig. 1) are known to be very efficient for sludge incineration [2], this study focuses on the modeling of these devices. Such models have already been derived both for coal combustion or gasification [3–10] as well as for biomass and sludge incineration or gasification [11–14]. One of the main drawbacks of these models is that the reactor is often considered as isothermal and/or to operate at stationary conditions. This is the reason why our final goal is to propose a detailed model able to catch all the information required by the prediction of transient incineration and gasification of sewage sludge. Such a model has already been derived in the case of incineration of municipal solid waste by Marias et al. [15,16]. One of the main interest of their model relies on a two-dimensional description of the film between the bubbles and the emulsion zone which allows a better estimation of volatile combustion and hence of the

\* Corresponding author. Tel.: +33 559 407 809; fax: +33 559 407 801.  
E-mail addresses: Frederic.marias@univ-pau.fr (F. Marias),  
fethi.zagrouba@isste.rnu.tn (F. Zagrouba).

**Nomenclature**

$a$	specific area of the bed ( $\text{m}^{-1}$ )
$A_{\text{ech}}$	total exchange area in the bed ( $\text{m}^2$ )
$A_c$	cross-sectional surface of the bed ( $\text{m}^2$ )
$c_{p_i}$	constant pressure specific heat of $i$ ( $\text{J kg}^{-1} \text{K}^{-1}$ )
$D$	diffusion coefficient ( $\text{m}^2 \text{s}^{-1}$ )
$F_1$	mass flow rate in the carry over (slag) ( $\text{kg s}^{-1}$ )
$F_2$	mass flow rate elutriated (ashes) ( $\text{kg s}^{-1}$ )
$f$	auxiliary function
$h$	heat exchange coefficient ( $\text{W m}^{-2}$ )
$h_{f,i}^\circ$	standard enthalpy of formation of $i$ ( $\text{J kg}^{-1}$ )
$h_{\text{rp}}$	heat exchange coefficient of reactive particles ( $\text{W m}^{-2}$ )
$h_{\text{sd}}$	heat exchange coefficient of sand ( $\text{W m}^{-2}$ )
$H$	total enthalpy ( $\text{J kg}^{-1}$ )
$K$	equilibrium constant
$L^{\text{bed}}$	expanded bed height (m)
$L^{\text{dis}}$	height of the disengagement zone
$L^{\text{post}}$	height of the post-combustion zone
$\dot{m}_0$	mass flow rate of carbon particle in the equivalent input ( $\text{kg s}^{-1}$ )
$\dot{m}_{\text{air,sec}}$	mass flow rate of secondary air ( $\text{kg s}^{-1}$ )
$\dot{m}_{\text{gas}}$	mass flow rate of auxiliary gas ( $\text{kg s}^{-1}$ )
$\dot{m}_{\text{vol}}$	mass flow rate of volatiles issued from pyrolysis of waste ( $\text{kg s}^{-1}$ )
$M$	molar weight ( $\text{kg mol}^{-1}$ )
$P_0$	Atmospheric pressure (Pa)
$r$	carbon particle radius (m)
$R$	chemical reaction rate ( $\text{kg m}^{-3} \text{s}^{-1}$ ) or enthalpy reaction rate ( $\text{J m}^{-3} \text{s}^{-1}$ )
$\bar{R}_s$	average specific reaction rate for a carbon particle inside the bed ( $\text{kg m}^{-2} \text{s}^{-1}$ )
$T$	absolute temperature (K)
$T_a$	temperature of the air (K)
$T_c$	temperature of reactive particles (K)
$T_{\text{ref}}$	reference temperature (298 K)
$U_0$	superficial fluidization velocity at ambient conditions ( $\text{m s}^{-1}$ )
$U(z)$	superficial velocity inside bubble zone ( $\text{m s}^{-1}$ )
$U_1$	equivalent fluidization velocity ( $\text{m s}^{-1}$ )
$U_{\text{mf}}$	incipient fluidization velocity ( $\text{m s}^{-1}$ )
$W_c$	total mass of reactive particles (carbon) within the furnace (kg)
$y$	transversal space co-ordinate in the buffer zone (m)
$Y$	chemical species mass fraction
$z$	height above the distributor (m)
$Z$	chemical element mass fraction

*Greek symbols*

$\alpha_{\text{rp}}$	ratio of mass of carbon in the disengaging zone to bed one
$\alpha_{\text{sd}}$	ratio of mass of sand in the disengaging zone to bed one

$\beta$	ratio of mass flow rate of volatile released in the disengagement zone
$\gamma$	ratio of mass flow rate of secondary air released in the disengagement zone
$\delta$	buffer zone thickness (m)
$\varepsilon_b$	volume fraction of the bed occupied by bubbles
$\varepsilon_d$	porosity in the disengaging zone
$\varepsilon_{\text{mf}}$	porosity at incipient fluidization
$\Delta_r H$	enthalpy of reaction ( $\text{J kg}^{-1}$ )
$\Lambda$	coefficient in the heterogeneous reaction
$\xi$	arbitrary variable (either mass fraction or total enthalpy to weight)
$\varphi$	carbon particle size distribution in the furnace ( $\text{m}^{-1}$ )
$\varphi_0$	initial waste particle size distribution ( $\text{m}^{-1}$ )
$\varphi_{\text{vol}}$	specific mass flow-rate of volatiles from emulsion to buffer ( $\text{kg m}^{-2} \text{s}^{-1}$ )
$\rho_{\text{emul}}$	density of gas in the emulsion zone ( $\text{kg m}^{-3}$ )
$\omega$	rate of shrinkage of reactive particles ( $\text{m s}^{-1}$ )

*Subscripts*

rp	relative to reactive particle
c	relative to carbon

*Superscripts*

Air	relative to air
bub	relative to bubble zone
buff	relative to buffer zone
dis	relative to disengaging zone
emul	relative to emulsion zone
gas	relative to extra-gas
post	relative to post combustion zone
vol	relative to volatile matter

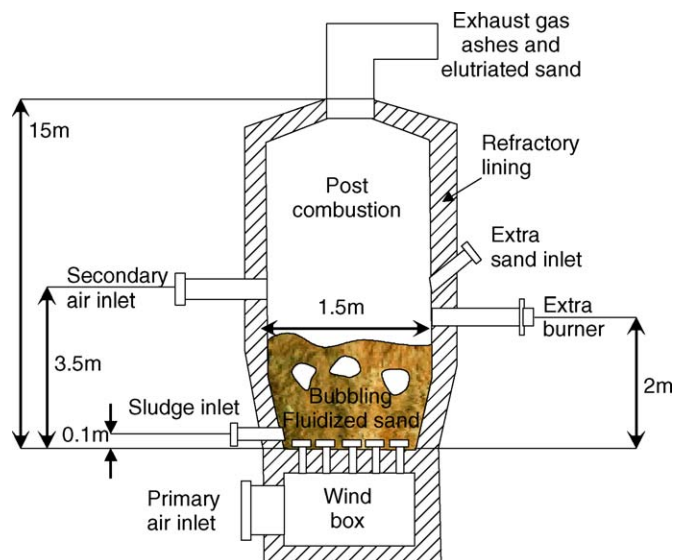


Fig. 1. Fluidized bed reactor (unscaled sketch).

maximal temperature reached within the incinerator. This model is being modified in order to predict fluidized bed incineration of sewage sludge. This paper presents its energetic preliminary validation. More precisely, the choice has been made to test the ability of the model to compute limit moisture contents of the incoming sludge compatible with operating temperature of the incinerator.

In a first section, the main features of the model are presented as well as the main assumptions it relies on. Then, in a second section, the ability of the model to compute moisture content limits for self-incineration of three different types of sludge: primary sludge, activated sludge and digested sludge, is discussed. Given their proximate and ultimate analysis as well as their lower heating values, two limits have been computed:

- the lower one corresponds to the minimal temperature of 850 °C that must prevail within the furnace in order to satisfy environmental regulation and to achieve complete combustion of sludge;
- the higher one is linked to the melting point of flying ashes. Indeed, above 1100 °C, ashes are expected to melt and then to stick on the wall of the furnace, what could, damage its refractory lining.

The results of the model are tested in comparison to results obtained assuming the fluidized bed incinerator to be a completely stirred tank reactor (CSTR) and to data from the literature. Moreover, some transient results are presented to show the ability of the model to simulate the start up of a unit.

## 2. Mathematical modeling

As it has been quoted in the introduction, many models have been developed for the fluidized bed combustion (or gasification) of char as well as for biomass and sludge. Some of these models deal with circulating fluidized bed combustion, which is an extension of conventional fluidization technology. However, there is still a need for the mathematical modeling of the in-depth bed.

### 2.1. Hydrodynamic model

According to a hydrodynamic point of view, most of the models in literature describe the dense bed by a two phases system [17,18]: a bubble phase (free of solids and undergoing plug flow conditions) and an emulsion phase (which might be either a completely stirred tank reactor or a plug flow, with axial dispersion or not). Transfer between these two phases is computed from global transfer coefficients that can be evaluated according to appropriate correlations [19]. The modeling approach presented in this paper is slightly different and should better describe the situation where sludge is fed inside the bed. In this case, an important part of the volatiles are expected to be released within the emulsion zone. In bubbling regime, the main part of the primary air crosses the bed as bubbles surrounded by the emulsion. Consequently, there is a zone surrounding the bubbles where diffusional combustion occurs. It is precisely in this region that

the maximal temperatures, which can be encountered within the bed, are expected to prevail. Tracking of these high temperature zones is very important to simulate the production of pollutants that are under kinetic control. Nitrogen oxides fall within this category. When heat and mass transfer between emulsion and bubbles is predicted according to global transfer coefficients (two phases' theory), such a tracking is not possible. To take into account these different aspects, a third zone (the buffer zone) [15,16,18] is considered. It was described as a two-dimensional region where both transport under diffusion and convection processes occur and allowed a more accurate description of the bed behavior during the process.

The freeboard of the bed is described by two completely stirred tank reactors. The first one corresponds to the transport disengagement height. Its thermal level and chemical composition depends on the presence of solid particles (sand and reactive particles). The second one corresponds to the post combustion zone, which is located above the disengagement region. It is completely free of solids. Figs. 2 and 3 give further information on this hydrodynamic modeling.

### 2.2. Assumptions for the model

The following assumptions are made for the model:

- the mass of sand present in the bed is supposed to be constant during the operation;
- the sewage sludge and primary air are fed at the bottom of the Bubbling Fluidized Bed Combustor (BFBC);
- the auxiliary fuel (propane  $C_3H_8$ ), is injected in the disengagement zone at a mass flow-rate  $\dot{m}_{gas}$ ;
- secondary air is supposed to be distributed over disengagement and post combustion as follows:
  - $\gamma \dot{m}_{air,sec}$  in the disengagement;
  - $(1 - \gamma) \dot{m}_{air,sec}$  in the post-combustion.

The value of the parameter  $\gamma$  depends on the position of the secondary air supply inside the incinerator.

- external heat power is added or removed to the bed in order to keep it at 850 °C or 1100 °C;

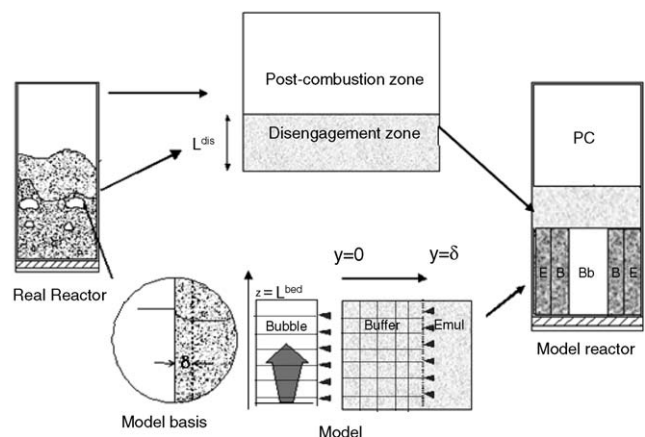


Fig. 2. Sketch of the model zones.

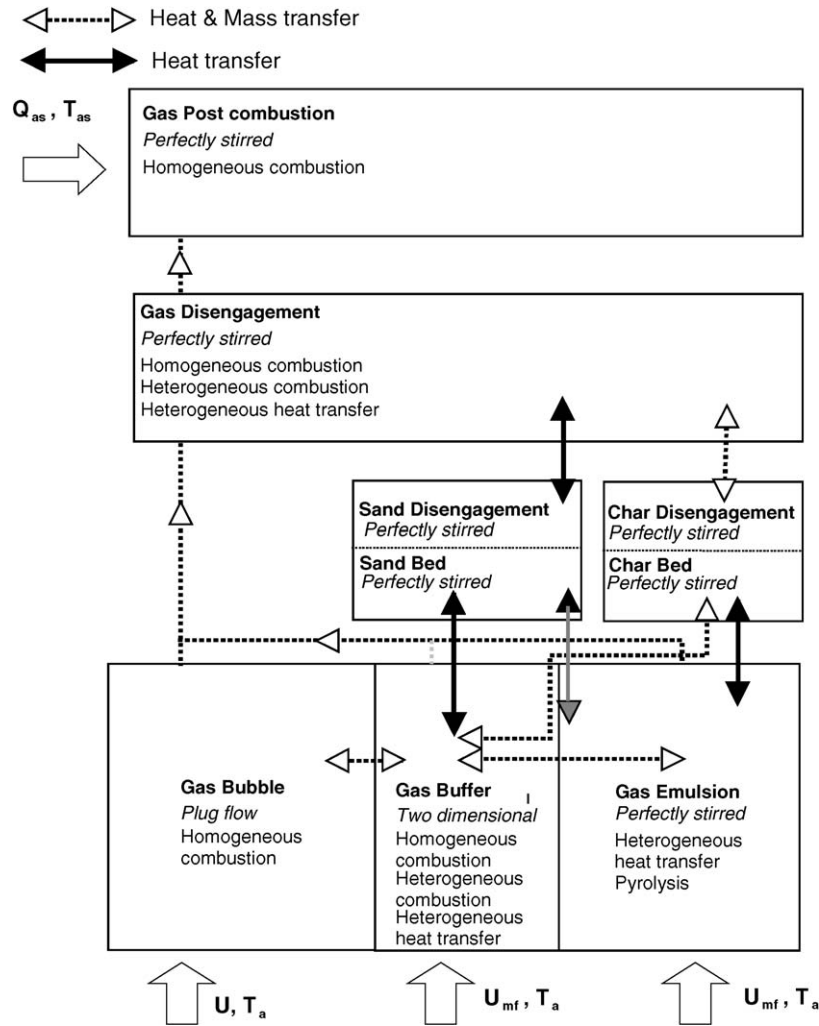


Fig. 3. Overall reactor model.

- mass flow rate of sludge is fixed in order to obtain 6% of  $O_2$  in the post combustion zone.

Flash pyrolysis is still the main assumption made in the scope of this work. The following paragraph is dedicated to this step.

### 2.3. Flash pyrolysis

Because of the high heating rates that prevail within fluidized beds, and according to numerous authors [11,12,20–30], a flash pyrolysis of sludge is assumed to occur as soon as the waste enters the reactor. Thus, given the proximate analysis of the sludge under consideration, the particle of sludge is assumed to be instantaneously decomposed into its moisture fraction, its volatilisable fraction, particles of pure carbon (corresponding to the fixed carbon content of the sludge) and ashes, respectively.

The high heating value gas [2–16,20–30] is composed of light hydrocarbons and pollutants, which are released in both emulsion and disengagement. More precisely, if we suppose that  $\beta$  represents the fraction of volatiles released within the disengagement and  $\dot{m}_{vol}$  the total mass flow rate of volatile matter, then

the specific mass flow of volatiles drained out of the emulsion (in order to keep it in incipient fluidization conditions) towards the bubbles is expressed as:

$$\varphi_{vol} = \frac{(1 - \beta)\dot{m}_{vol}}{aA_c L^{bed}} \quad (1)$$

The composition of the volatiles is computed from atomic balances given the ultimate analysis of the sludge [16].

Besides, the flash pyrolysis is supposed to keep the distribution size of sludge [11,14,16], i.e. the size distribution of the reactive particles (issued from pyrolysis and composed of pure carbon) is the same that the one of the original waste particles ( $\varphi_0$ ).

### 2.4. Governing equations

The main mathematical equations describing the model are the following:

#### 2.4.1. Emulsion zone

The gas in the emulsion phase is expected to be perfectly stirred. This is the region where a part of the heat transfer with

reactive and inert particles takes place and where flash pyrolysis occurs, influencing the release of the volatiles. In fact, some of the volatiles are released within this zone (whereas, the other part is released at the top of the bed). Because the emulsion zone is kept at incipient fluidization conditions, the gas arising from the flash pyrolysis of sludge inside the emulsion must be drained out of this zone. This is the reason why a net flow of gas exists from the emulsion towards the bubble.

Using the assumption of perfect mixing within this part of the reactor, the mass and energy conservation equations within the zone we derived under the following form:

$$A_c \varepsilon_{mf} \frac{\partial \rho_{emul}(1 - \varepsilon_b - a\delta)L^{bed} \xi^{emul}}{\partial t} = \rho^{emul} A_c (1 - a\delta) U_{mf} [\xi^{air} - \xi^{emul}] + (1 - \beta) \dot{m}_{vol} [\xi^{vol} - \xi^{emul}] - \rho^{emul} D \iint_{A_{ech}} \left. \frac{\partial \xi^{buff}}{\partial y} \right|_{y=\delta} dA + A_c L^{bed} (1 - \varepsilon_b - a\delta) \varepsilon_{mf} R_{\xi}^{emul} \quad (2)$$

where  $\xi^{emul}$  stands for a state variable under inspection (mass fraction of element, enthalpy) in the emulsion phase.

This equation states that accumulation of  $\xi$  within the volume  $A_c L^{bed} (1 - \varepsilon_b - a\delta) \varepsilon_{mf}$  of gas, held within the emulsion, is balanced by:

- the entering of  $\xi$  from the fluidizing air:  $\rho_{emul} A_c (1 - a\delta) U_{mf} \xi^{air}$ ;
- the entering of  $\xi$  by the volatiles:  $(1 - \beta) \dot{m}_{vol} \xi^{vol}$ ;
- the gas leaving the zone by ascending and transversal flow (fluidizing air and volatiles from emulsion to bubble):  $[\rho_{emul} A_c (1 - a\delta) U_{mf} + (1 - \beta) \dot{m}_{vol}] \xi^{emul}$ ;
- the diffusive transfer of  $\xi$  at the boundary of the buffer zone:  $-\rho_{emul} D \iint_{A_{ech}} \left. \frac{\partial^2 \xi^{buff}}{\partial y} \right|_{y=\delta}$ ;
- the production of  $\xi$  within the zone:  $A_c L^{bed} (1 - \varepsilon_b - a\delta) \varepsilon_{mf} R_{\xi}^{emul}$ ;
- The source term  $R_{\xi}^{emul}$  is computed as follows:
  - zero for all chemical element  $Z_k^{emul}$ , except  $Z_C^{emul}$ ;
  - value depending upon reaction of reactive particles of pure carbon for  $Z_C^{emul}$ ;
  - value imposed by kinetics data for  $Y_{NO}^{emul}$  and  $Y_{HCN}^{emul}$ ;
  - sum of exchange terms with the in-bed boiler (if present) and solid particles held within the zone and value depending upon heterogeneous reaction of reactive particles inside the zone for  $H^{emul}$ .

#### 2.4.2. Buffer zone

The conservation of the elements and enthalpy in the buffer zone is described by a two-dimensional parabolic convection diffusion equation where the diffusion takes place only in the  $y$  direction (the high value of the Peclet number in the  $z$  direction

leads to pure convection in this direction).

$$\varepsilon_{mf} \frac{\partial \rho_{emul} a \xi^{buff}}{\partial t} = -\rho_{emul} a U_{mf} \frac{\partial \xi^{buff}}{\partial z} + \varphi_{vol} a \frac{\partial \xi^{buff}}{\partial y} + \rho_{emul} a D \frac{\partial^2 \xi^{buff}}{\partial y^2} + \varepsilon_{mf} a R_{\xi}^{buff} \quad (3)$$

where  $\xi^{buff}$  represents the state variable under consideration.

This equation is obtained using balances over a volume of gas  $a A_c \varepsilon_{mf} dy dz$  inside the buffer:

- $A_c dy dz \varepsilon_{mf} \frac{\partial \rho_{emul} a \xi^{buff}}{\partial t}$  stands for accumulation of  $\xi$  within the infinitesimal volume;
- $\rho_{emul} a A_c U_{mf} dy (\xi^{buff}(z) - \xi^{buff}(z + dz)) = -\rho_{emul} a A_c U_{mf} dy dz \frac{\partial \xi^{buff}}{\partial z}$  stands for the net transport of  $\xi$  by ascending fluidizing air;
- $\varphi_{vol} a A_c dz (\xi^{buff}(y + dy) - \xi^{buff}(y)) = \varphi_{vol} a A_c dz dy \frac{\partial \xi^{buff}}{\partial y}$  stands for the net transport of  $\xi$  by the transversal flow of volatiles from emulsion to bubbles;
- $-\rho_{emul} a A_c dz D \left( \left. \frac{\partial \xi^{buff}}{\partial y} \right|_y - \left. \frac{\partial \xi^{buff}}{\partial y} \right|_{y+dy} \right) = \rho_{emul} a A_c dz dy D \frac{\partial^2 \xi^{buff}}{\partial y^2}$  stands for the net transport of  $\xi$  by diffusion;
- $a A_c \varepsilon_{mf} dy dz R_{\xi}^{buff}$  represents the source term of  $\xi$  within the volume; The value of the source term  $R_{\xi}^{buff}$  is:
  - zero for all chemical elements  $Z_k^{buff}$ , except  $Z_C^{buff}$ ;
  - depending upon reaction of reactive particles of pure carbon for  $Z_C^{buff}$ ;
  - imposed by kinetics data for  $Y_{NO}^{buff}$  and  $Y_{HCN}^{buff}$ ;
  - the sum of exchange terms with solid particles held within the volume and value depending upon heterogeneous reaction of reactive particles inside the volume for  $H^{buff}$ .

#### 2.4.3. Bubble zone

Assuming plug flow within this solid free region, the transport of chemical elements and enthalpy is governed by a one-dimensional equation:

$$\frac{\partial \varepsilon_b \rho_{emul} \xi^{bub}}{\partial t} = -\rho_{emul} \left[ \frac{\partial U \xi^{bub}}{\partial z} \right] + a \varphi_{vol} \xi^{buff} \Big|_{z,y=0} + \rho_{emul} a D \left. \frac{\partial \xi^{buff}}{\partial y} \right|_{z,y=0} + \varepsilon_b R_{\xi}^{bub} \quad (4)$$

where:

$$U(z) = U_1 - U_{mf} + \frac{(1 - \beta) \dot{m}_{vol} z}{\rho_{emul} A_c L^{bed}} \quad (5)$$

Eq. (4) is obtained using balances over a control volume of gas  $A_c \varepsilon_b dz$  inside the bubble zone:

- $A_c dz \frac{\partial \rho_{emul} \varepsilon_b \xi^{bub}}{\partial t}$  stands for accumulation of  $\xi$  inside the volume;

- $A_c \rho_{\text{emul}}(U(z)\xi^{\text{bub}}(z) - U(z + dz)\xi^{\text{bub}}(z + dz)) = -A_c \rho_{\text{emul}} dz \frac{\partial U \xi^{\text{bub}}}{\partial z}$  stands for net transport of  $\xi$  by ascending fluidizing air inside the volume;
- $a A_c dz \varphi_{\text{vol}} \xi^{\text{buff}}|_{z,y=0}$  represents the supply of  $\xi$  by the transversal flow of volatiles from emulsion to bubble;
- $\rho_{\text{emul}} a D \frac{\partial \xi^{\text{buff}}}{\partial y}|_{z,y=0}$  represents the supply of  $\xi$  by diffusion at the boundary of the buffer zone;
- $A_c \varepsilon_b dz R_{\xi}^{\text{bub}}$  stands for the source term of  $\xi$  inside the volume:
  - it is zero for all chemical element  $Z_k^{\text{bub}}$  (no solid particles inside the volume);
  - its value imposed by kinetics data for  $Y_{\text{NO}}^{\text{bub}}$  and  $Y_{\text{HCN}}^{\text{bub}}$ ;
  - it is zero for  $H^{\text{bub}}$  (no solid particles inside the volume).

Eq. (5) is obtained using a global mass balance over the same volume. The function  $U$  introduced stands for the superficial velocity of gas within the bubbles.

#### 2.4.4. Disengagement

The solid material present in this zone originates from bursting of bubbles at the top of the dense bed [23]. The presence of sand and particles implies heterogeneous transfers and reactions that affect greatly the global conversion rate.

Supposed to be a completely stirred tank reactor, disengagement is described by the following equation for enthalpy and elements:

$$\varepsilon_d \frac{\partial \rho_{\text{emul}} L^{\text{dis}} \xi^{\text{dis}}}{\partial t} = \rho_{\text{emul}} U(L^{\text{bed}}) \xi^{\text{bub}}|_{z=L^{\text{bed}}} + a \rho_{\text{emul}} U_{\text{mf}} \int_0^{\delta} \xi^{\text{buff}}(y, L^{\text{bed}}) dy + (1 - a\delta) \rho_{\text{emul}} U_{\text{mf}} \xi^{\text{emul}} + \frac{\beta \dot{m}_{\text{vol}}}{A_c} \xi^{\text{vol}} + \gamma \frac{\dot{m}_{\text{air,sec}}}{A_c} \xi^{\text{air}} + \frac{\dot{m}_{\text{gas}}}{A_c} \xi^{\text{gas}} + L^{\text{dis}} \varepsilon_d R_{\xi}^{\text{dis}} - \left( \rho_{\text{emul}}(U(L^{\text{bed}}) + U_{\text{mf}}) + \frac{\beta \dot{m}_{\text{vol}}}{A_c} + \gamma \frac{\dot{m}_{\text{air,sec}}}{A_c} + \frac{\dot{m}_{\text{gas}}}{A_c} \right) \xi^{\text{dis}} \quad (6)$$

This equation is obtained using a balance over the volume of gas  $A_c \varepsilon_d L^{\text{dis}}$  held within the zone:

- $A_c \varepsilon_d \frac{\partial \rho_{\text{emul}} L^{\text{dis}} \xi^{\text{dis}}}{\partial t}$  represents the accumulation of  $\xi$  within the disengagement;
- $A_c \rho_{\text{emul}} U(L^{\text{bed}}) \xi^{\text{bub}}|_{z=L^{\text{bed}}}$  stands for the supply of  $\xi$  by the gas issuing from the bubble zone;
- $A_c a \rho_{\text{emul}} U_{\text{mf}} \int_0^{\delta} \xi^{\text{buff}}(y, L^{\text{bed}}) dy$  denotes the supply of  $\xi$  by the gas issuing from the buffer zone;
- $A_c (1 - a\delta) \rho_{\text{emul}} U_{\text{mf}} \xi^{\text{emul}}$  stands for the supply of  $\xi$  by the gas issuing from the emulsion zone;
- $\beta \dot{m}_{\text{vol}} \xi^{\text{vol}}$  accounts for the supply of  $\xi$  by the volatiles released within the zone;
- $\gamma \dot{m}_{\text{air,sec}} \xi^{\text{air}}$  stands for the supply of  $\xi$  by the secondary air;
- $\dot{m}_{\text{gas}} \xi^{\text{gas}}$  represents the supply of  $\xi$  by the auxiliary gas;
- $(A_c \rho_{\text{emul}}(U(L^{\text{bed}}) + U_{\text{mf}}) + \beta \dot{m}_{\text{vol}} + \gamma \dot{m}_{\text{air,sec}} + \dot{m}_{\text{gas}}) \xi^{\text{dis}}$  represents the transport of  $\xi$  by the flow leaving the zone;
- $A_c L^{\text{dis}} \varepsilon_d R_{\xi}^{\text{dis}}$  stands for the source term of  $\xi$  within the zone:
  - it is zero for all chemical element  $Z_k^{\text{dis}}$ , except  $Z_{\text{C}}^{\text{dis}}$ . In this last case, it is depending upon reaction of reactive particles of pure carbon for  $Z_{\text{C}}^{\text{dis}}$ ;
  - it is imposed by kinetics data for  $Y_{\text{NO}}^{\text{dis}}$  and  $Y_{\text{HCN}}^{\text{dis}}$ ;
  - it is given by the sum of exchange terms with solid particles held within the zone and value depending upon hetero-

geneous reaction of reactive particles inside the zone for  $H^{\text{dis}}$ .

#### 2.4.5. Post-combustion zone

This zone is the upper part of the freeboard (free of solids) and where different homogenous reactions occur. The assumption of complete mixing within this region leads to the following equation:

$$A_c \frac{\partial \rho_{\text{fuel}} L^{\text{post}} \xi^{\text{post}}}{\partial t} = (A_c \rho_{\text{emul}}(U(L^{\text{bed}}) + U_{\text{mf}}) + \beta \dot{m}_{\text{vol}} + \gamma \dot{m}_{\text{air,sec}} + \dot{m}_{\text{gas}}) [\xi^{\text{dis}} - \xi^{\text{post}}] + (1 - \gamma) \dot{m}_{\text{air,sec}} [\xi^{\text{air}} - \xi^{\text{post}}] + A_c L^{\text{post}} R_{\xi}^{\text{post}} \quad (7)$$

This equation is obtained using a balance over the volume of gas  $A_c L^{\text{post}}$  held in the post-combustion zone:

- $A_c \frac{\partial \rho_{\text{fuel}} L^{\text{post}} \xi^{\text{post}}}{\partial t}$  stands for accumulation of  $\xi$  in the zone;
- $(A_c \rho_{\text{emul}}(U(L^{\text{bed}}) + U_{\text{mf}}) + \beta \dot{m}_{\text{vol}} + \gamma \dot{m}_{\text{air,sec}} + \dot{m}_{\text{gas}}) \xi^{\text{dis}}$  stands for supply of  $\xi$  from the disengagement;
- $(1 - \gamma) \dot{m}_{\text{air,sec}} \xi^{\text{air}}$  accounts for the supply of  $\xi$  by the secondary air;

- $(A_c \rho_{\text{emul}}(U(L^{\text{bed}}) + U_{\text{mf}}) + \beta \dot{m}_{\text{vol}} + \gamma \dot{m}_{\text{air,sec}} + \dot{m}_{\text{gas}} + (1 - \gamma) \dot{m}_{\text{air,sec}}) \xi^{\text{post}}$  represents the output of  $\xi$  from the zone;
- $A_c L^{\text{post}} R_{\xi}^{\text{post}}$  stands for the source term of  $\xi$  in the zone:
  - it is zero for all chemical element  $Z_k^{\text{post}}$  (no solid particles inside the volume);
  - it is imposed by kinetics data for  $Y_{\text{NO}}^{\text{post}}$  and  $Y_{\text{HCN}}^{\text{post}}$ ;
  - it is zero for  $H^{\text{post}}$  (no solid particles).

#### 2.4.6. Reactive particles

The particle size distribution function is computed as the solution of the following equation, which is obtained from a population balance of particles that range between  $r$  and  $r + dr$ :

$$\frac{\partial W_c \varphi}{\partial t} = \dot{m}_0 \varphi_0 - F_1 \varphi - F_2 \varphi - W_c \frac{\partial \omega \varphi}{\partial r} + 3 \frac{W_c \varphi \omega}{r} \quad (8)$$

where  $\varphi$  represents the distribution function (on a mass basis),  $W_c$  the total mass of reactive particles held inside the furnace, and  $\omega$  is the rate of shrinkage of a single particle (computed using both kinetics and mass transfer limitation). The evaluation of this last datum requires the knowledge of the particle temperature, which is computed using an enthalpy balance over a single particle (as seen later in this paragraph).

The different terms arising in Eq. (8) have the following signification:

- $\frac{\partial W_c \varphi}{\partial t} dr$  stands for the accumulation of mass particle inside the range  $r, r + dr$ ;
- $\dot{m}_0 \varphi_0$  represents the supply of mass of particle inside the range under consideration by the pyrolysis of waste (residue of fixed carbon);
- $(F_1 + F_2) \varphi dr$  accounts for the output of mass of particles by carry-over and elutriation;
- $W_c (\omega(r, t) \varphi(r, t) - \omega(r + dr, t) \varphi(r + dr, t)) = -W_c dr \frac{\partial \omega \varphi}{\partial r}$  stands for the net increase of mass of particles by their input and output of the range  $r, r + dr$ ;
- $3 \frac{W_c \varphi \omega}{r} dr$  disappearance of mass of solid particles because of heterogeneous reaction inside the range (the term  $\omega$  is negative).

In this last term,  $\omega$  is the average rate of shrinkage of particle depending upon external mass transfer of oxygen at the surface of the particle and kinetics of the reaction (heterogeneous reaction  $C_{(s)} + \Delta O_2 \rightarrow (2 - 2\Delta)CO + (2\Delta - 1)CO_2$ ).

The temperature is the solution of the following non-linear ordinary differential equation (energy balance equation over a particle of radius  $r$ ) assuming equal-probability of presence of reactive particles over the emulsion, the buffer zone and the disengagement zone.

$$\frac{4}{3} \pi r^3 \frac{\partial \rho_c c_{p_c} T_c}{\partial t} = - \left[ (1 - \alpha_{rp}) \frac{a\delta}{(1 - \varepsilon_b)} \bar{R}_s^{\text{buff}} + \alpha_{rp} R_s^{\text{dis}} \right] 4\pi r^2 \Delta_r H_C + \alpha_{rp} h_{rp} (T^{\text{dis}} - T_c) 4\pi r^2 + (1 - \alpha_{rp}) \frac{a\delta 4\pi r^2}{(1 - \varepsilon_b)} h_{rp}(r, t) \times (\bar{T}^{\text{buff}} - T_c) + (1 - \alpha_{rp}) h_{rp} (T^{\text{emul}} - T_c) \frac{(1 - \varepsilon_b - a\delta)}{(1 - \varepsilon_b)} 4\pi r^2 \quad (9)$$

The preceding equation states that accumulation of heat by the particle is due to heterogeneous reaction (within the buffer and the disengagement,  $R_s^{\text{zone}}$  stands for the local rate of reaction within each zone) and exchange with gas held in the disengagement, the buffer (represented by an average temperature  $\bar{T}^{\text{buff}}$ ) and the emulsion zone. Parameter  $W\alpha_{rp}$  stands for the mass of reactive particles present in the disengagement zone while  $W(1 - \alpha_{rp})$  represents the mass of reactive particles present within the buffer and emulsion zones. This value is computed according to the work of Marias et al. [15,16]. Indeed, a mass flow rate of solid particles brought to the freeboard of the bed by the bursting of bubbles is computed. Then, assuming that they are brought back to the bed at their terminal velocity, one is able to compute the residence time of the particles inside the freeboard. The evaluation of their mass is simply performed dividing the mass flow rate of solid particles brought to the bed by their residence time inside the bed.

In Eq. (9),  $h_{rp}$  stands for the total heat transfer coefficient between solid reactive particles and bubbles. It was estimated by the correlations proposed by Prins [19] for both convective and radiative heat transfer within a hot fluidized bed of sand.

Finally, to normalize the size distribution, the following integral equation is required:

$$\int_0^\infty \varphi(r, t) dr = 1 \quad (10)$$

#### 2.4.7. Boundary conditions

The following spatial boundary conditions must apply for the buffer:

$$\begin{aligned} \xi^{\text{buff}}(y = 0, z, t) &= \xi^{\text{bub}}(z, t); & \xi^{\text{buff}}(y = \delta, z, t) &= \xi^{\text{emul}}(t); \\ \xi^{\text{buff}}(y, z = 0, t) &= \xi^{\text{air}}(t) \end{aligned} \quad (11)$$

As  $L^{\text{bed}}$  and  $\delta$  depend on the temperature and chemical composition of the emulsion (which both highly change with time), right and upper boundaries ( $z = L^{\text{bed}}, y = \delta$ ) behave as “moving” boundaries.

The following boundary condition applies for the bubble:

$$\xi^{\text{bub}}(z = 0, t) = \xi^{\text{air}}(t) \quad (12)$$

The mathematical modeling of a fluidized bed reactor must not be limited to this hydrodynamic description of the bed. Indeed, specific issues such as drying, pyrolysis, char burn out, and combustion of the volatiles have to be addressed. Dealing with chemistry of the system, chemical equilibrium is supposed to be reached for  $O_2, N_2, CH_4, H_2, H_2O, CO, CO_2, C_6H_6, HCl, Cl_2, SO_2, SO_3, H_2S$  inside the gas held within each region, whereas,  $NO$  and  $HCN$  are supposed to be under kinetic control. A specific post treatment is used to compute  $NO$  production both by thermal and fuel bound mechanisms.

Finally, the size distribution of particles of pure carbon is computed assuming that their reaction rate is controlled both by kinetics and by oxygen transfer to the surface of the particle.

Some more algebraic equations are required to evaluate both the different source terms occurring within the differential equations and the bed properties. All these complementary equations were already presented by Marias et al. [15,16]. The scope of this paper is not to present the whole model but to give the reader some information about the way it is set-up (interested reader should refer to these papers).

### 3. Model results

#### 3.1. Energetic model validation

Numerous computations have been carried out to predict the limit of moisture content in terms of auto-combustion and safe processing (no damage of the reactor) for different sludges (primary sludge, activated sludge and digested sludge). These limits have been fixed on a lower and a higher thermal level, which are 850 and 1100 °C, respectively. A temperature of 850 °C is required in order to complete combustion of the sludge, and to satisfy environmental regulation. The limit of 1100 °C is relative to the melting of flying ashes that could stick to the wall of the furnace and damage it. To ensure nominal processing con-

Table 1  
Analyses of the sludge under consideration

	Primary sludge	Activated sludge	Digested sludge
Proximate analysis (wt.%)			
Moisture (raw)	To be determined	To be determined	To be determined
Ash (db)	0.35	0.23	0.50
Volatiles (daf)	0.65	0.77	0.50
Fixed carbon (daf)	0	0	0
Lower heating value ( $\text{J kg}^{-1}$ dry)	$15.12 \times 10^6$	$17.28 \times 10^6$	$10.8 \times 10^6$
Ultimate analysis (wt.% daf)			
C	51.5%	53%	49%
H	7%	6.7%	7.7%
O	35.5%	33%	35%
N	4.5%	6.3%	6.2%
S	1.5%	1%	2.1%

Table 2  
Computed values for moisture content and air in excess to reach  $850^\circ\text{C}$  in post combustion

	Primary sludge	Activated sludge	Digested sludge
Moisture (raw, %)	62.6	63.5	51
Air in excess (%)	45.8	38.8	39.9
Computed temperature ( $^\circ\text{C}$ )	855	847	855
Computed $\text{O}_2$ (%)	6.06	5.91	6.06

ditions, the secondary air-flow rate has been adjusted in order to keep a value of 6% of  $\text{O}_2$  in the post combustion. Characteristics of the considered sludges are reported in Table 1, whereas, computations results are presented in Tables 2 and 3. These tables yield the two upper quoted limits as well as the ratios of air in excess that have been used to reach the specification of oxygen content in the post combustion.

Because of its conception, the model has been set-up to compute operating conditions (temperature, composition, particle size distribution . . .) for a given set of operating parameters (mass flow rate of sludge, of air, moisture content of sludge . . .). In this paper, the operating parameters are needed in order to fulfill a set of operating conditions. Consequently, successive runs have been done to reach the desired conditions. Because they are not exactly 6% of  $\text{O}_2$  and  $850^\circ\text{C}$  (or  $1100^\circ\text{C}$ ), the exact value of oxygen content and temperature in the post combustion zone that have been computed and reported for any sludge under consideration.

In a goal of comparison, the researched parameters (moisture content and ratio of air in excess) have been computed by a

Table 3  
Computed values for moisture content and air in excess to reach  $1100^\circ\text{C}$  in post combustion

	Primary sludge	Activated sludge	Digested sludge
Moisture (raw, %)	50.1	52.0	33.75
Air in excess (%)	44.6	41.0	41.1
Computed temperature ( $^\circ\text{C}$ )	1120	1108	1098
Computed $\text{O}_2$ (%)	6.02	6.00	5.85

simpler approach, which considers fluidized bed incinerator as a completely stirred tank reactor. For this computation, it is also assumed that carbon, hydrogen, nitrogen and sulfur are completely converted to carbon dioxide, water, nitrogen oxide and sulfur dioxide. A global mass balance, a balance on chemical element oxygen and an energy balance yield the limit moistures as well as the corresponding air in excess. Table 4 summarizes the results obtained from this simplified computation.

First of all it can be verified that the buffer-zone model gives good predictions for the moisture content corresponding to self-incineration. Indeed, the dryness of primary, activated and digested sludges reported by OTV [31] from industrial data are 42.5%, 37% and 45.5%, whereas, the model predicts 37.4%, 36.5% and 49%, respectively. The values, which should not be exceeded have been estimated from the model to 49.9%, 48%, and 66.25%, respectively. The highest dryness (either for lower limit or for upper limit) is reached in the case of the digested sludge, which has the lower heating value.

The results also indicate that, for every kind of sludge under consideration, approximately 40% of air in excess should be brought to the furnace to reach environmental regulation.

The results predicted by both the detailed model and the simplified approach show very good agreement for the two limits of moisture content. However, some slight differences on the prediction of the air in excess (that should be supplied to the furnace) can be noted. This discrepancy arises from the difference

Table 4  
Results of the simplified CSTR computation

	$T^{\text{post}} = 850^\circ\text{C}$ , $y_{\text{O}_2}^{\text{post}} = 6\%$	$T^{\text{post}} = 1100^\circ\text{C}$ , $y_{\text{O}_2}^{\text{post}} = 6\%$
Primary sludge		
Moisture (raw, %)	62.2	50.1
Air in excess (%)	53.2	48.1
Activated sludge		
Moisture (raw, %)	64.1	50.9
Air in excess (%)	51.1	46.5
Digested sludge		
Moisture (raw, %)	50.7	35.4
Air in excess (%)	49.7	45.7



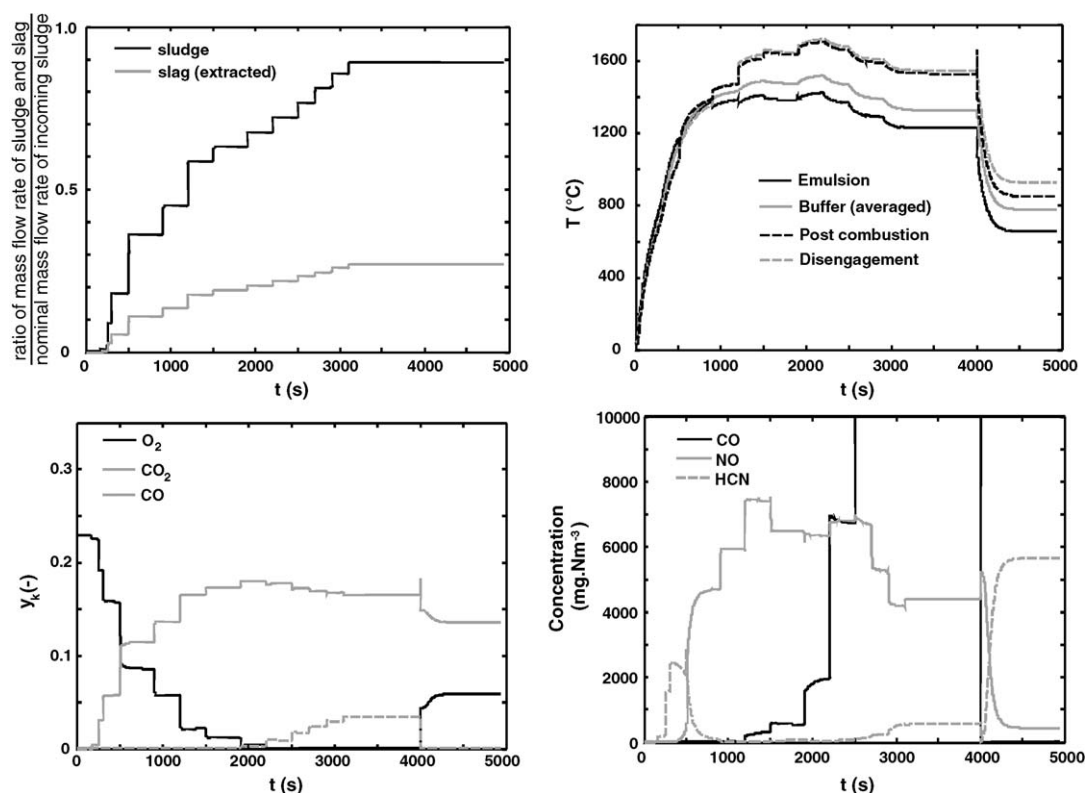


Fig. 4. Transient simulation of the start up of the fluidized bed with auxiliary gas. Lately shut down of extra gas. Upper left: evolution of ratio of mass flow rate of sludge fed to the bed and slag extracted from the bed to nominal mass fraction of incoming sludge; upper right: evolution of temperatures inside the reactor; lower left: mass fraction of species at the output of the furnace (post combustion); lower right: mass concentration of species at the output of the furnace (post combustion).

for the prediction of chemical reactions. Indeed, in the simplified CSTR model, all the carbon and hydrogen are expected to be fully oxidized to carbon dioxide and water. In a different way, the buffer-zone model is based on chemical equilibrium computations. Consequently, a part of the carbon can be released as carbon monoxide and a part of the moisture content (of the sludge) can be converted to hydrogen following water gas shift reaction  $\text{CO} + \text{H}_2\text{O} \leftrightarrow \text{CO}_2 + \text{H}_2$ . This limits the requirements of oxygen from the incoming air, because some oxygen is transferred from the water content of the sludge. These phenomena lead to a decrease in the air requirements and explain the difference between the two model predictions.

### 3.2. Transient model results

The presented model also allows transient predictions. The effects of the modification of an operating parameter can be checked not only on the final set of operating conditions but also on the transient ones. Fig. 4 illustrates such results that could be obtained at the start up of a unit. More precisely, some extra gas is used in order to raise the temperature of the incinerator before the processing of sludge (activated sludge). But, in this example of start up, the extra gas is shut down too late (4000 s) and the secondary air-flow rate is not sufficient to keep the oxygen level up to 6% in the post combustion zone. The extra gas leads to overly high temperature levels in the reactor (one can notice that the furnace is not isothermal and that the highest temperatures are expected to occur within the disengagement zone). The first

impact of these high temperatures is the high value of carbon monoxide production. Indeed, because chemical equilibrium is assumed, the high temperatures lead to the dissociation of carbon dioxide into oxygen and carbon monoxide. Then when the temperature is decreased and when secondary air is added to the system at 4000 s in order to reach the legal 6% of oxygen in the post combustion, the carbon monoxide is wholly converted to carbon dioxide. The second effect of these high temperatures is relative to the high values of the nitric oxide emissions: above 1100 °C (500 s) the whole part of the fuel bound nitrogen is converted to NO while it is kept into HCN below this value. Finally, the stationary conditions are reached and for a moisture content of 63.5% on raw basis, the temperature of the post combustion is stabilized at 850 °C. These results show good qualitative agreement to what can be expected. However, this model has to be fully tested before being used intensively.

## 4. Conclusion

A detailed model for the fluidized bed incineration of sludge has been presented. It is able to compute composition of the gas held inside the furnace (in terms of  $\text{O}_2$ ,  $\text{N}_2$ ,  $\text{CH}_4$ ,  $\text{H}_2$ ,  $\text{H}_2\text{O}$ ,  $\text{CO}$ ,  $\text{CO}_2$ ,  $\text{C}_6\text{H}_6$ ,  $\text{HCl}$ ,  $\text{Cl}_2$ ,  $\text{SO}_2$ ,  $\text{SO}_3$ ,  $\text{H}_2\text{S}$ ,  $\text{NO}$ , and  $\text{HCN}$  mass fractions) the temperature and the particle size distribution of pyrolysis residue with respect to time. Its main characteristic is that the combustion of the volatiles at the surroundings of the bubbles is described by adding a third zone to the classical two-phases description of bubbling fluidized beds. Both the

main assumptions and the principal equations have been written. Results of a start up procedure have been presented in order to illustrate the ability of the model to accurately describe transient behavior. In the validation procedure of this model, preliminary studies have been performed. The limit values of the dryness of three different sludges have been computed. The lower limit corresponds to self-incineration, whereas, the upper one corresponds to maximal working temperature. The results are the following (in terms of dryness range):

- primary sludge: [42.5%; 49.9%];
- activated sludge: [37.0%; 48.0%];
- digested sludge: [45.5%; 66.3%].

The results show good agreement with the literature, at least for the prediction of the lower dryness. Moreover, this computation has been compared to the prediction of a simplified model that assumes the whole incinerator to be a completely stirred reactor, with complete oxidation of carbon, hydrogen, nitrogen and sulfur. The discrepancies between the two models show the importance of the prediction of the chemical reactions. Indeed, chemical equilibrium gives more accuracy and allows for better description of the chemistry of the system especially at high temperature.

## References

- [1] Eurostat. URL: <http://europa.eu.int/comm/eurostat/>.
- [2] J. Werther, T. Ogada, Sewage sludge combustion, *Progress Energy Comb. Sci.* 25 (1999) 55–116.
- [3] F. Preto, Studies and Modeling of Atmospheric Fluidized Bed Combustion of Coal, PhD Thesis, Queen's University at Kingston, 1987.
- [4] M.L. De Souza-Santos, Comprehensive modeling and simulation of fluidized bed boilers and gasifiers, *Fuel* 68 (1989) 1507–1521.
- [5] G. Brem, Mathematical Modeling of Coal Conversion Processes With Application to Atmospheric Fluidized Bed Combustion, PhD Thesis, Netherlands Organization for Applied Scientific Research, 1990.
- [6] J. Adanez, J.C. Abanades, Modeling of lignite combustion in atmospheric fluidized bed combustors. 1. Selection of submodels and sensitivity analysis, *Indus. Eng. Chem. Process Res. Dev.* 31 (1992) 2286–2295.
- [7] J. Adanez, J.C. Abanades, Modeling of lignite combustion in atmospheric fluidized bed combustors. 2. Model validation and simulation, *Indus. Eng. Chem. Process Res. Dev.* 31 (1992) 2296–2304.
- [8] K.W. Junk, R.C. Brown, A model of coal combustion dynamics in a fluidized bed combustor, *Comb. Flame* 95 (1993) 219–228.
- [9] J. Hannes, Mathematical Modeling of Circulating Fluidized Bed Combustion, PhD Thesis, T.U. Delft, The Netherlands, 1996.
- [10] S. Sriramulu, S. Sane, P. Agarwal, T. Mathews, Mathematical modeling of fluidized bed combustion. 1. Combustion of carbon in bubbling beds, *Fuel* 75 (1996) 1351–1362.
- [11] H. Jaing, R.V. Morey, A numerical model of a fluidized bed biomass gasifier, *Biomass Bioenergy* 3 (1992) 431–447.
- [12] J.F. Bilodeau, N. Thérien, P. Proulx, S. Czernick, E. Chornet, A mathematical model of fluidized bed biomass gasification, *Can. J. Chem. Eng.* 71 (1993) 549–557.
- [13] J. Corella, A. Sanz, Modeling circulating fluidized bed biomass gasifiers. A pseudo-rigorous model for stationary state, *Fuel Process. Technol.* 86 (2005) 1021–1053.
- [14] I. Petersen, J. Werter, Experimental investigation and modeling of gasification of sewage sludge in the circulating fluidized bed, *Chem. Eng. Process.* 44 (2005) 717–736.
- [15] F. Marias, J.R. Puiggali, G. Flamant, Modeling for simulation of fluidized-bed incineration process, *AIChE J.* 47 (2001) 1438–1460.
- [16] F. Marias, J.R. Puiggali, G. Flamant, Effects of freeboard volatile release during fluidized bed incineration of a model waste, *Trans. Inst. Chem. Eng., Part B: Process Safety Environ. Protect.* 79 (2001) 244–252.
- [17] D. Kunii, O. Levenspiel, *Fluidization Engineering*, 2nd ed., Butterworth-Heinemann Series in Chemical Engineering, Boston, 1991.
- [18] I. Braianov, F. Marias, J.M. Renaume, Dynamic simulation of a fluidized bed incineration process, *J. Comput. Meth. Sci. Eng.*, in press.
- [19] W. Prins, Fluidized Bed Combustion of a Single Carbon Particle, PhD Thesis, University of Twente, 1987.
- [20] S.R. Beck, M.J. Wang, Wood gasification in a fluidized bed, *Indus. Eng. Chem. Process Design Dev.* 19 (1980) 312–317.
- [21] F. Shafizadeh, Introduction to pyrolysis of biomass, *J. Anal. Appl. Pyrol.* 3 (1982) 283–305.
- [22] L. El Ghezal, Contribution à l'étude de la pyrolyse rapide et de la vapogazéification de sciure de bois dans un réacteur à lit fluidisé de sable chaud, PhD Thesis, Institut National Polytechnique de Toulouse, France, 1983.
- [23] R.G. Graham, M.A. Bergougnou, Fast pyrolysis of biomass, *J. Anal. Appl. Pyrol.* 6 (1984) 95–135.
- [24] M. Hemati, Etude de la pyrolyse et de la gazéification de bois par thermogravimétrie et en lit fluidisé de catalyseur, PhD Thesis, Institut National Polytechnique de Toulouse, France, 1984.
- [25] B. Dif, Pyrolyse-gazéification de la biomasse: Conception et mise au point d'un réacteur à lit fluidisé, PhD Thesis, Institut National Polytechnique de Lorraine, France, 1987.
- [26] L. Shen, D. Zhang, Low-temperature pyrolysis of sewage sludge and putrescible garbage for fuel oil production, *Fuel* 84 (2005) 809–815.
- [27] P. Piskorz, D.S. Scott, I.B. Westerberg, Flash pyrolysis of sewage sludge, *Indus. Eng. Chem. Process Res. Dev.* 25 (1986) 265–272.
- [28] G. Gasco, C.G. Blanco, F. Guerrero, A.M. Mendez Lazaro, The influence of organic matter on sewage sludge pyrolysis, *J. Anal. Appl. Pyrol.* 74 (2005) 413–420.
- [29] M.F. Gomez-Rico, I. Martín-Gullon, A. Fullana, J.A. Conesa, R. Font, Pyrolysis and combustion kinetics and emissions of waste lube oils, *J. Anal. Appl. Pyrol.* 68/69 (2003) 527–546.
- [30] R. Font, A. Fullana, J.A. Conesa, Kinetic models for the pyrolysis and combustion of two types of sewage sludge, *J. Anal. Appl. Pyrol.* 74 (2005) 429–438.
- [31] OTV, Traiter et valoriser les boues, Lavoisier Tec et Doc, Cachan, France, 1997.